Flight-Test Determination of Aircraft Cruise Characteristics Using Acceleration and Deceleration Techniques

T.R. Yechout*
U.S. Air Force Academy, Colorado Springs, Colorado

A flight-test technique has been developed under NASA Dryden sponsorship NSG 4028 to predict aircraft cruise performance characteristics. The technique used acceleration and deceleration maneuvers to define baseline aerodynamic and propulsion system characteristics, which were then input to a performance modeling prediction program. Conventional stabilized "speed power" tests, which are normally used for cruise performance definition, can comprise a large portion of the flight time in a program. A significant reduction in flight time was estimated using the performance modeling approach with associated savings in cost and schedule. A 20 h verification flight-test program was accomplished using a Learjet Model 35 aircraft.

Nomenclature

a	= speed of sound
a_x, a_z	= acceleration along x and z wind axes, respectively
C_D	= drag coefficient
C_{D_S}	= drag coefficient standardized for skin friction
C_L	= lift coefficient
C_{L_S}	= lift coefficient corrected for thrust moment effect and nonstandard center of gravity
C_{L_T}	= lift coefficient corrected for thrust moment effect
D	= drag
F_g	= gross thrust
F_r	= ram drag
F_x, F_z	= forces along x and z wind axes, respectively
g	= acceleration of gravity
L	= lift
M	= Mach number
m	= aircraft mass
N	= power of δ_{t_2} required to eliminate altitude dependency of corrected fuel flow
N_1	= low-pressure fan rpm
n_x, n_z	= x and z wind axes load factors, respectively
P	= ambient pressure
S	= wing reference area
S.L.	= sea level
t_2	= total property at the engine compressor face
V	= true velocity
W	= aircraft weight
W_a, W_f	= air and fuel flows, respectively
x, z	= longitudinal and normal axes, respectively
α	= angle of attack
γ	= flight-path angle
γ'	= ratio of specific heat for air
δ	= pressure ratio
η	= correction parameter for actual vs deck thrust specific fuel consumption
θ	= temperature ratio
λ	= thrust inclination angle
ρ	= air density

Received Sept. 23, 1986; revision received Sept. 15, 1987. This paper is declared a work of the U.S. Government and is not subject to copyright protection in the United States.

*Associate Professor, Department of Aeronautics. Member AIAA.

Introduction

A LARGE number of flight-test hours are required to define the performance characteristics of modern aircraft using classical flight-test techniques. Typically, cruise performance is defined by generating extensive speed-power data, whereas specific excess power and flight trajectory performance is defined from acceleration, climb, and descent tests throughout the flight envelope. A flight-test approach has been developed that requires a limited amount of acceleration/deceleration (quasisteady-state maneuvering) data to predict the overall 1 g cruise performance characteristics of an aircraft. A substantial savings in flight hours was realized when compared with the stabilized point method. In addition, this approach resulted in definition of baseline aircraft and engine performance characteristics allowing flexible applications to a variety of situations such as aircraft simulation.

Concept

The first step in developing an overall aircraft performance model was the definition of baseline aerodynamic and propulsion system characteristics. Baseline aerodynamic characteristics consisted primarily of the lift and drag models, whereas baseline engine characteristics included the gross thrust, fuel flow, and airflow models. Development of lift and drag characteristics from quasisteady-state maneuvers began with consideration of the forces acting on the aircraft. The aircraft force balance equations, resolved parallel and perpendicular to the flight path (assuming zero sideslip, wings level, and constant mass) are, from Fig. 1:

$$\Sigma F_x = ma_x$$

$$\Sigma F_z = ma_z$$

$$F_g \cos(\alpha+\lambda) - F_r - D = W(a_x/g + \sin\gamma)$$

$$L + F_g \sin(\alpha+\lambda) = W(a_z/g + \cos\gamma)$$

As discussed in Ref. 1, the flight-path load factors resolved along the x and z wind axes are

$$n_x = a_x/g + \sin\gamma$$

$$n_z = a_z/g + \cos\gamma$$

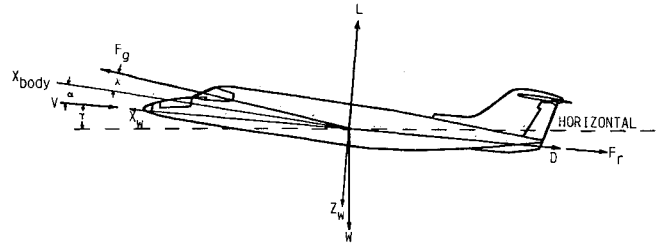

Fig. 1 Aircraft force diagram.

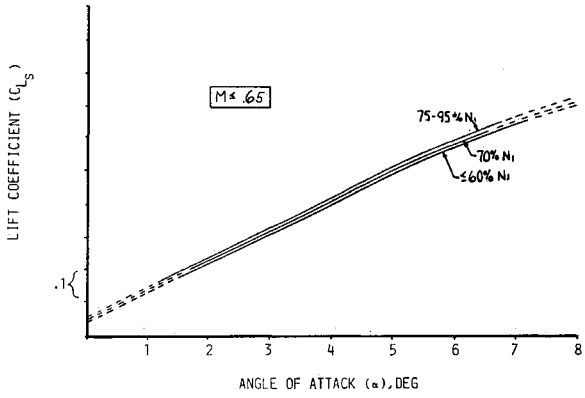

Fig. 2 Lift coefficient characteristics, $M \leq 0.65$.

The force balance equations may then be expressed as

$$F_g \cos(\alpha+\lambda) - F_r - D = Wn_x$$

$$L + F_g \sin(\alpha+\lambda) = Wn_z$$

These equations can easily be used to express lift and drag coefficients in terms of wind axis accelerations, the engine parameters of gross thrust and ram drag, and normally recorded flight-test parameters such as angle of attack, ambient pressure, weight, and Mach number.

$$C_L = \frac{Wn_z - F_g \sin(\alpha+\lambda)}{\frac{1}{2}\gamma' PM^2 S} \tag{1}$$

$$C_D = \frac{F_g \cos(\alpha+\gamma) - F_r - Wn_x}{\frac{1}{2}\gamma' PM^2 S} \tag{2}$$

The equations are compatible with quasisteady-state maneuvers where excess thrust is not equal to zero and flight-path accelerations are present. Wind axis accelerations were determined from accelerometers mounted along the body axis of the aircraft using the appropriate angular transformations. A complete development of these relationships is presented in Ref. 2, including corrections to lift coefficient for elevator trim effects resulting from 1) the thrust moment about the center of gravity (c.g.), and 2) a nonstandard c.g. and a correction to drag coefficient for skin friction variation as a function of Reynolds number.

A new dimension of this program concerned in-flight definition of the aerodynamic effect of thrust level on lift and drag characteristics. Normally, lift and drag measurements are accomplished using a series of stabilized points throughout the aircraft flight envelope. A wide range of engine power settings are used to achieve the stabilized conditions from which lift and drag may be determined, given an in-flight thrust and airflow model along with normally instrumented aircraft parameters such as weight and angle of attack. Unfortunately, the flowfield around the aircraft may be significantly altered by the airflow through the engine(s), which will result in the lift and drag characteristics being directly dependent on engine power. If the stabilized point method is used on an aircraft where power effects are significant, use of the resulting data to predict nonstabilized (i.e., excess thrust not equal to zero) performance characteristics will be susceptible to significant error. As a result, a technique was developed to evaluate the effect of engine power setting on lift and drag characteristics. A complete development of this technique is presented in Ref. 3.

Level acceleration and deceleration maneuvers at various power settings were performed across the Mach range of the aircraft to define lift coefficient and drag coefficient data as a function of power setting and Mach number. The needed lift coefficient range was obtained through a variation of the weight-pressure ratio (W/δ). The power-dependent effects were defined by comparing data for the same Mach number and angle of attack. Significant power effects were identified for both lift and drag using this technique on the Learjet 35, which should be anticipated for any aircraft with jet engines mounted on the aft fuselage above the inboard wing section. An example of lift coefficient results from the low Mach regime is presented in Fig. 2, showing the power effect as a function of engine fan rpm (N_1).

The in-flight engine model consisted of 1) corrected thrust (F_g/δ_{t_2}), 2) corrected fuel flow ($W_f/\sqrt{\theta_{t_2}}\delta_{t2}^N$), and 3) corrected airflow airflow ($W_a\theta_{t_2}/\delta_{t_2}$), which were calculated and plotted vs corrected rpm ($N_1\sqrt{\theta_{t_2}}$) at constant Mach number. A unique in-flight thrust and airflow prediction technique, termed "thrust modeling," was developed to define these parameters. This technique provided several advantages over other methods, including: 1) easy implementation into on-line data reduction software, 2) relatively limited and easily installed engine instrumentation, and 3) improved accuracy over methods that rely completely on engine deck prediction. The technique consisted of correcting the engine deck predictions of thrust and airflow to match the performance of the actual engines installed in the aircraft using a three-step approach: 1) simplified representation of engine deck predicted thrust, fuel flow, and airflow in corrected form, 2) correction of the engine deck model, developed in step 1, to the individual characteristics of each engine based on a static thrust run, and 3) in-flight correction of thrust and airflow predictions based on actual test fuel flow, an accurate specific fuel consumption prediction and balance of the thrust momentum equation.

The final equations in simplified form for thrust and airflow are

$$F_{g_{\text{in-flight}}} = \frac{W_{f_{\text{in-flight}}} F_{g_{\text{deck}}}}{nW_{f_{\text{deck}}}} \tag{3}$$

$$W_{a_{\text{in-flight}}} = W_{f_{\text{in-flight}}} \left[\frac{W_{a_{\text{deck}}}}{\eta W_{f_{\text{deck}}}} + \frac{1}{\eta} - 1 \right] \tag{4}$$

where η is the ratio of static thrust run specific fuel consumption to engine deck specific fuel consumption, defined as a function of corrected rpm. A complete development of this technique is presented in Ref. 4. Thrust and airflow prediction accuracies were believed to be 3–5% or better based on data obtained from past flight-test programs. F_g and W_a were then put in corrected form and input to the in-flight engine model.

The baseline aircraft/engine characteristics formed the basis for predicting aircraft cruise performance. These characteristics were utilized in a prediction program for this purpose. The program calculated steady-state cruise performance in terms of corrected rpm, range factor (RF), specific range (SR), and specific range parameter (SRP) vs Mach for constant values of W/δ. Since steady-state performance parameters could not be explicitly solved for, an iterative

routine was developed that would converge upon the steady-state solution. This routine iterated on lift coefficient to obtain steady-state values of C_D, C_L, F_g, F_r, α, SR, SRP, RF, and $N_1\sqrt{\theta_{t_2}}$ at a constant W/δ for the entire Mach envelope.

The routine normally started with desired steady-state values of W/δ, altitude, fan rpm (N_1), and Mach number. The iteration first approximated lift coefficient with the equation

$$C_L = W/\delta\left(\frac{2}{P_{\text{S.L.}}\gamma' M^2 S}\right) \tag{5}$$

However, this value of lift coefficient did not take into account thrust or thrust moment effects and was, therefore, not a steady-state value. The iteration routine next calculated aircraft angle of attack based on the last approximation of lift coefficient. This was accomplished with a table lookup of the baseline C_{L_S} vs α characteristics.

With angle of attack defined, the drag coefficient could be determined. Drag over delta was then calculated with

$$D/\delta = \frac{C_D\gamma' P_{\text{S.L.}} SM^2}{2}$$

A table lookup for test engine airflow was performed, using corrected rpm and Mach number. Corrected ram drag was calculated with

$$\frac{F_r}{\delta_{t_2}} = \frac{W_a V/g}{\delta_{t_2}} = \left[\frac{W_a\sqrt{\theta_{t_2}}/\delta_{t_2} M_a}{\sqrt{\theta_{t_2}} g}\right]$$

where a is the local speed of sound, and $W_\alpha\sqrt{\theta_{t_2}}/\delta_{t_2}$ is the corrected airflow from the table lookup. The above ram drag calculation was for one engine and was multiplied by 2 to represent the combined total of both engines for the Lear 35. At the same time, the total pressure correction was multiplied out, yielding F_r/δ, which was used to calculate gross thrust in the next step. With the values of drag over delta and ram drag over delta defined, the gross thrust over delta could then be calculated:

$$F_g/\delta = \frac{D/\delta + F_r/\delta}{\cos(\alpha+\lambda)}$$

and the corrected thrust was

$$F_g/\delta_{t_2} = \frac{F_g/\delta}{(1+0.2M^2)^{3.5} x\text{PRF}}$$

where PRF is the engine inlet pressure recovery factor. Next, a new power level N_1 was defined. This was accomplished using the baseline gross thrust model F_g/δ_{t_2} vs $N_1/\sqrt{\theta_{t_2}}$ and M.

Finally, the lift coefficient was updated

$$C_L = \frac{W/\delta - (F_g/\delta)\sin(\alpha+\lambda)}{\frac{1}{2}\gamma' P_{\text{S.L.}} SM^2}$$

and corrected for thrust moment effect and c.g. position

$$C_{L_T} = C_L + \Delta C_{L_{\text{thrust moment}}}$$

$$C_{L_S} = C_{L_T} + \Delta C_{L_{\text{c.g.}}}$$

With two lift coefficients defined, a test for convergence was performed. For the first iteration, a comparison of the approximated C_L [Eq. (5)] to the value of C_{L_S} computed with the above equation was made. If convergence was not achieved, C_L was set equal to C_{L_S}, and the iteration continued with a new calculation of angle of attack. Agreement between the last iteration and the present iteration was required to be within +0.00001 for convergence. When the lift coefficient did converge, the new steady-state values of C_{D_S}, C_{L_S}, F_g, F_r, range factor, specific range, specific range parameter, and $N_1/\sqrt{\theta_{t_2}}$ were stored. Mach number was then incremented and the iteration performed again. The process continued until the entire Mach envelope had been defined. A typical number of iterations for convergence was three. The range parameters were defined as:

$$\text{Range factor (RF)} = VW/W_f$$

$$\text{Specific range (SR)} = V/W_f$$

$$\text{Specific range paramter (SRP)} = V\delta/W_f$$

Test Procedure

Quasisteady-state acceleration/deceleration maneuvers provided the necessary data to define aerodynamic and propulsion characteristics. These maneuvers were conducted at nearly constant altitude using the altitude-hold mode of the autopilot. Normally, less than a 60 ft excursion from the start altitude was experienced during a maneuver. Eight "cardinal" power settings were evaluated consisting of 95, 90, 85, 80, 75, 70, 60, and 50% N_1. The N_1 was chosen as the variable to represent power because of the relatively high bypass ratio of the engines and the resulting high correlation to engine airflow. An acceleration/deceleration was conducted at a cardinal power setting by holding N_1 to within + 0.5% during a maneuver. A range of the weight-pressure ratio parameter (W/δ) within the aircraft envelope was designated to provide a lift coefficient variation for a given Mach number so that Mach effects could be defined. Eight values of W/δ were evaluated, as shown in Table 1. These eight values of W/δ provided eight evenly spaced points on a constant Mach drag polar in the mid-Mach range. At each value of W/δ, an acceleration/deceleration sequence was performed that included

Table 1 Performance modeling maneuvering sequences

W/δ (lb)	Nominal altitude, ft
22,000	10,000
40,000	23,000
47,000	26,000
53,000	29,000
60,000	32,000
67,000	35,000
73,000	38,000
80,000	40.000

Table 2 Maneuvering sequence

Sequence	Power setting	Maneuver	Data recorded
1	95	Accel	Yes
2	90	Decel	Yes
3	70	Decel	Yes
4	90	Accel	Yes
5	95	Accel	No
6	85	Decel	Yes
7	70	Decel	Yes
8	85	Accel	Yes
9	95	Accel	No
10	80	Decel	Yes
11	70	Decel	Yes
12	80	Accel	Yes
13	95	Accel	No
14	75	Decel	Yes
15	70	Decel	Yes
16	75	Accel	Yes

polar in the midMach range. At each value of W/δ, an acceleration/deceleration sequence was performed that included maneuvers at all cardinal power settings above idle. As W/δ increased, the number of available power settings decreased because the idle rpm increases with altitude. For example, at 40,000 ft only the 95, 90, and 85% power settings could be evaluated. As a result, the largest amount of data was obtained for the higher power settings.

A typical maneuvering sequence is illustrated in Fig. 3, which assumes the drag curve and engine idle level are as shown for a particular W/δ configuration. A sequence began by slowing the aircraft to an acceptable minimum speed (for the Lear 35 this was an airspeed slightly above stick shaker speed) at an altitude based on the target value of W/δ. A 95% acceleration was then performed. When the acceleration had slowed to approximately 0.25 knots/s, the throttles were retarded to 90% and a deceleration performed until a stabilized point was approached. The sequence then continued, as shown in Fig. 3 and Table 2. Altitude adjustments were made at convenient times in the sequence to maintain W/δ within approximately 1% as weight decreased. Although not specifically shown in Fig. 3, a high-power setting for sequence 9 was used to accelerate past the stabilized condition so that the deceleration as shown in sequence 10 could be obtained (Table 2). Although a stabilized speed-power point was generally not obtained, the Mach number for which the drag and net thrust curves intersected could easily be estimated based on Mach region where the acceleration and deceleration for a particlar power setting were terminated. The general guideline used was to accelerate far enough past the last stabilized condition so that the engine rpm would achieve stabilization on the subsequent deceleration before reaching the Mach number of the last stabilized point. Data were taken periodically throughout an acceleration/deceleration rather than continually to keep the volume of data to a manageable level.

Ideally, approximately a 20-s burst of data was recorded as the aircraft passed through each 0.05 Mach increment. The actual test sequence performed at each W/δ condition depended directly on the location of the drag curve with respect to the net thrust levels. For example, if two cardinal power settings were located between engine idle and the bottom of the drag curve, then at least one deceleration would be performed at each of these power settings. The maneuver sequence was designed to acquire the needed data in a time-efficient manner and also be easily accomplished by the flight crew. It clearly met these objectives. For planning purposes, approximately 45 min were required to accomplish a maneuvering sequence at one value of W/δ for this aircraft. Additional flight-time savings could easily have been achieved by reducing the number of cardinal power settings. Although slighly less resolution of power effects would result, the flight-time savings appear to more than justify the alternative.

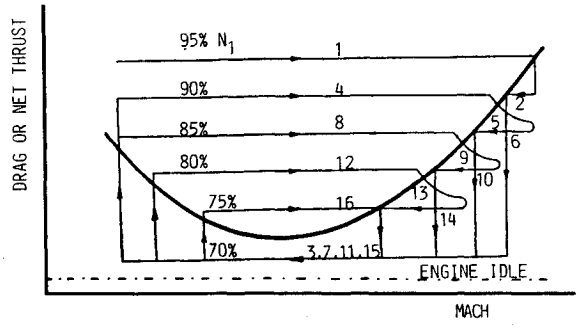

Fig. 3 Typical maneuvering sequence.

Results

A 20 h flight-test program was accomplished using a Learjet Model 35 aircraft to verify the technique. As a basis for comparison and evaluation of the modeling predictions, a total of 22 stabilized points were flown at four target values of W/δ (22,000, 40,000, 60,000, and 80,000 lb). The range factor data from the stabilized point tests were standardized using conventional techniques. The same four W/δ cases were evaluated with the modeling program. Figures 4–11 present the corrected rpm and range factor predictions generated as a function of Mach number. The stabilized point data is presented for comparison. Modeling prediction error bands of 5 and 10% are also included. The corrected rpm predictions generally were within 5% of the stabilized point data. Exceptions to this were in the low-speed region, where stabilized conditions are more difficult to achieve and cruise performance characteristics are of relatively low interest. For standardized range factor, the predictions were generally within 10% of the stabilized point data, with the lower W/δ cases experiencing better prediction correlation than the higher W/δ cases. For the 60,000 W/δ case, where approximately twice as many stabilized points were available, considerable scatter in the stabilized point data can be observed, which indicates that a significant error band is associated with definition of range factor when using exclusively stabilized point data, the currently accepted practice. Similar results were obtained for SR and SRP.

When evaluating the agreement between the predictions and stabilized point data, the error band associated with definition of the cruise characteristics using exclusively stabilized point data must be considered. This error band was estimated to be at least 5%, which was generally the same magnitude of error experienced when comparing the predictions and stabilized

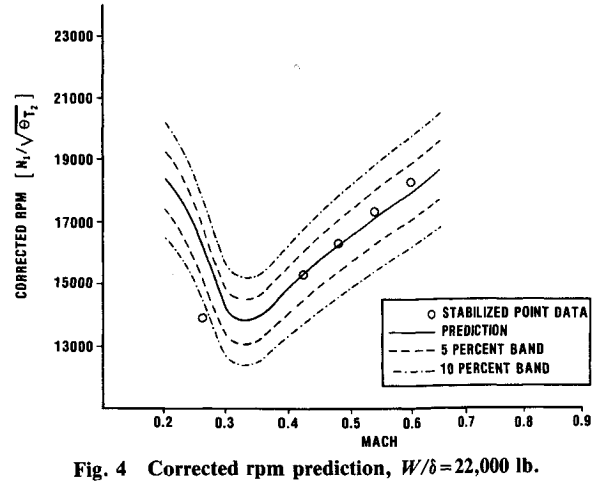

Fig. 4 Corrected rpm prediction, $W/\delta = 22{,}000$ lb.

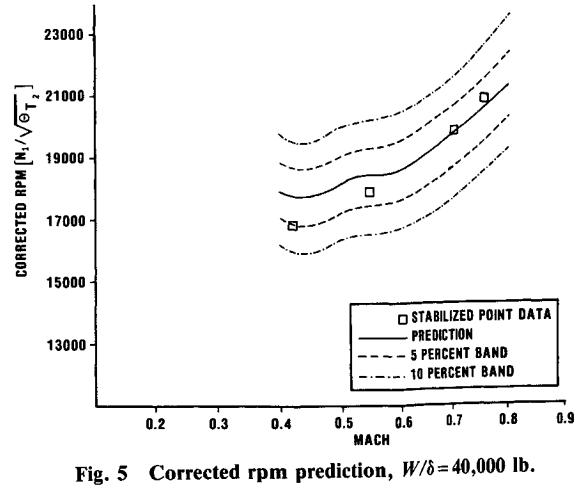

Fig. 5 Corrected rpm prediction, $W/\delta = 40{,}000$ lb.

Table 3 Sensitivity analysis summary

Baseline parameters	Error source	Instrumentation accuracy	Max relative error (%)	Max absolute error
C_{L_s}	$n_{z_{body}}$	±0.005 g	0.525	0.4×10^{-2}
	Dynamic pressure	±0.002 psi	0.364	0.291×10^{-2}
C_{D_4}	W_f	±10 lb/h	1.12	0.051×10^{-2}
	$n_{x_{body}}$	±0.001 g	1.26	0.056×10^{-2}
	$n_{z_{body}}$	±0.005 g	0.818	0.063×10^{-2}
	α	+0.1 deg	1.86	0.14×10^{-2}
	Dynamic pressure	±0.002 psi	0.355	0.027×10^{-2}
F_g/δ_{t_2}	N_1	±0.2%	0.448	16.56 lb
	W_f	±10 lb/h	1.97	73.6 lb
	Static pressure	±0.00075 psi	0.012	2.11 lb
	Dynamic pressure	±0.002 psi	0.07	1.74 lb
$W_a\sqrt{\theta_{t_2}}/\delta_{t_2}$	N_1	±0.2%	0.665	0.85 lb/s
	W_f	±10 lb/h	2.01	2.37 lb/s
	Static pressure	±0.00075 psi	0.12	0.015 lb/s
	Dynamic pressure	±0.001 psi	0.07	0.096 lb/s
F_g	N_1	±0.2%	0.308	8.42 lb
	W_f	±10 lb/h	2.05	40.3 lb
	Static pressure	±0.00075 psi	0.007	0.139 lb
	Dynamic pressure	±0.002 psi	0.098	2.24 lb
W_a	N_1	±0.2%	0.297	0.505 lb/s
	W_f	±10 lb/h	2.01	2.16 lb/s
	Static pressure	±0.00075 psi	0.007	0.0077 lb/s
	Dynamic pressure	±0.002 psi	0.082	0.104 lb/s

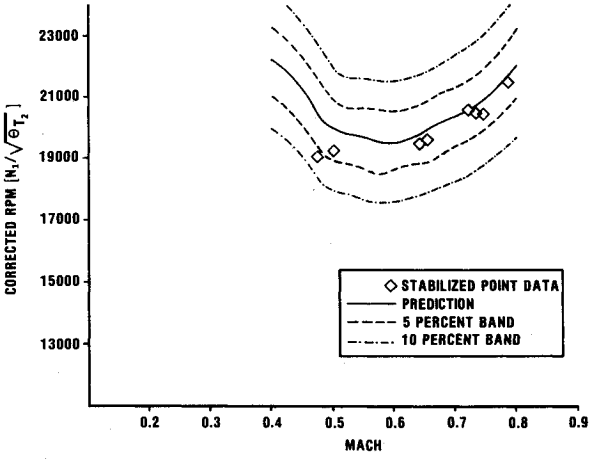

Fig. 6 Corrected rpm prediction, $W/\delta = 60{,}000$ lb.

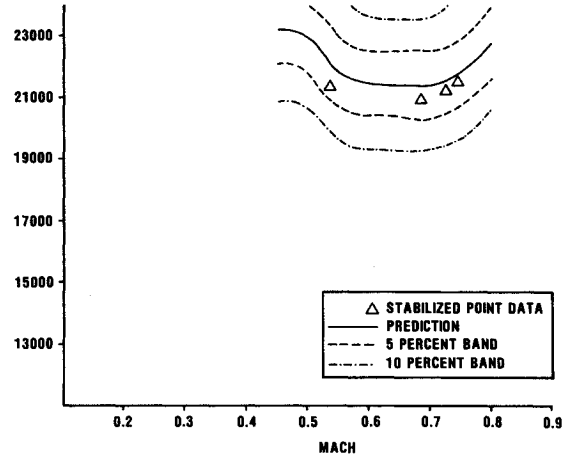

Fig. 7 Corrected rpm prediction, $W/\delta = 80{,}000$ lb.

point data. In view of this, the prediction correlation achieved was considered acceptable.

A sensitivity analysis was accomplished to identify the most critical instrumentation parameters affecting definition of baseline aerodynamic and engine characteristics. The actual accuracies of instrumentation transducers used during the program formed the basis for the analysis. The accuracy of each transducer was at or near state-of-the-art values. Table 3 presents the results of this analysis. The maximum absolute and relative error was determined for each of the baseline parameters listed as a function of critical instrumentation transducers. The maximum induced error for each instrumentation parameter was based on its associated accuracy. The body accelerations, angle of attack, and fuel flow were identified as having the largest error contributions for the aerodynamic characteristics. Fuel flow was the primary source of error for the engine characteristics. Fuel flow was identified as a critical prameter for both the aerodynamic and engine characteristics due to its direct relationship to gross thrust and airflow prediction used in the thrust modeling approach. [cf. Eq. (3) and (4)]. Since the instrumentation accuracies of the body accelerations, angle of attack, and fuel flow were at or

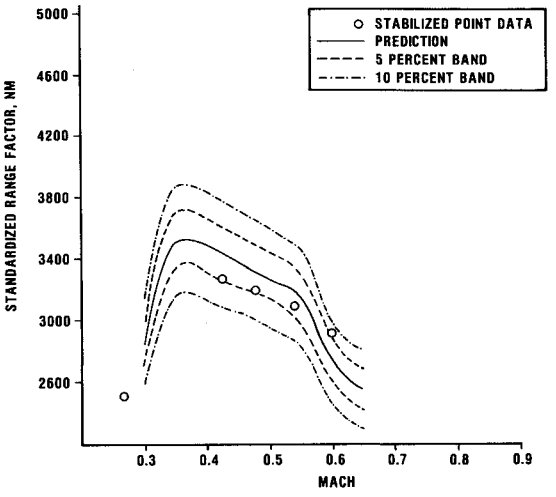

Fig. 8 Range factor prediction, $W/\delta = 22{,}000$ lb.

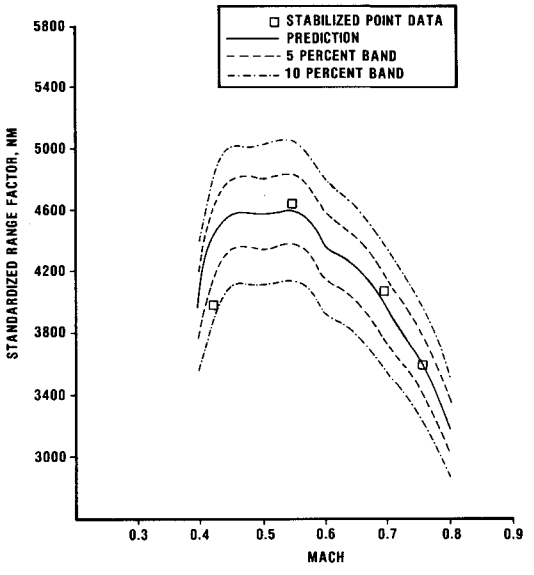

Fig. 9 Range factor prediction, $W/\delta = 40{,}000$ lb.

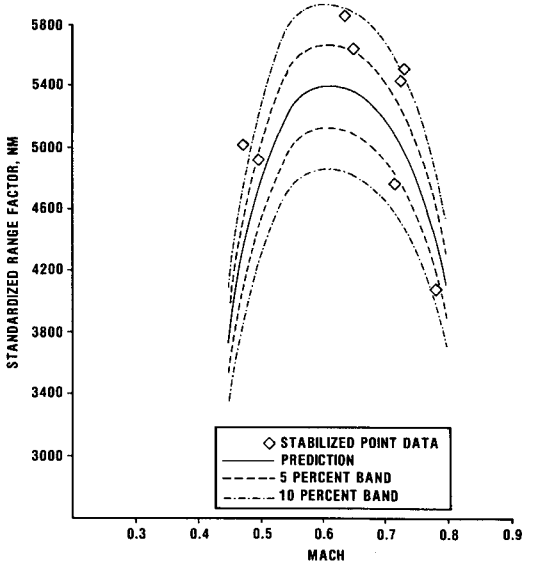

Fig. 10 Range factor prediction, $W/\delta = 60{,}000$ lb.

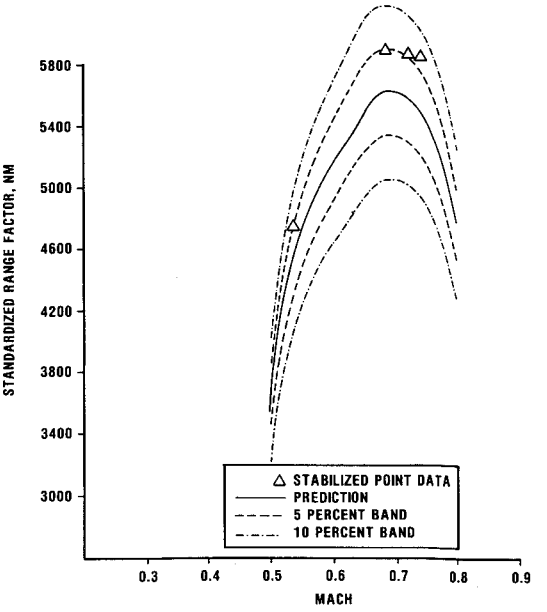

Fig. 11 Range factor prediction, $W/\delta = 80{,}000$ lb.

near state-of-the-art values, these parameters will have a significant influence on the errors associated with any performance modeling flight-test effort. Special attention should be given to obtaining state-of-the-art accuracies for these parameters if the performance modeling approach is used.

A significant reduction in flight-test time was projected using the performance modeling approach when compared to the more conventional stabilized point method. estimates for the Learjet 35 showed a savings in flight time of between 22 and 60% with the associated savings in cost and schedule. In addition, considerably more information was obtained along with the ability to predict performance characteristics for a wide variety of flight conditions.

Conclusions

A flight-test approach was developed to predict aircraft cruise performance using acceleration and deceleration maneuvers. Baseline aerodynamic and engine characteristics were defined and then input into a steady-state performance prediction program to estimate cruise characteristics such as RF, SR, SRP, and cruise engine rpm. A verification flight-test program using the Learjet 35 aircraft showed agreement generally to within 5% between the performance modeling predictions and stabilized point flight-test data. A significant savings in flight-test time was estimated using this approach.

Acknowledgments

The author wishes to express his appreciation to William G. Schweikhard and Keith B. Braman for their assistance with data reduction and analysis.

References

[1]Simpson, W.R., "The Accelerometer Methods of Obtaining Aircraft Performance from Flight Test Data," Center for Naval Analysis, Alexandria, VA, Professional Paper 245, June 1979, pp. 2–15.

[2]Yechout, T.R., "Modeling of Aircraft Performance From Flight Test Results Using Quasi Steady-State Test Techniques," Ph.D. Dissertation, Univ. of Kansas, Lawrence, KS, Jan. 1984, pp. 25–34.

[3]Yechout, T.R., Schweikhard, W.G., and Braman, K.B., "Flight Test Evaluation of Engine Power Effects on Lift and Drag," *Journal of Aircraft*, Vol. 22, May 1985, pp. 409–414.

[4]Braman, K.B., Schweikhard, W.G., and Yechout, T.R., "Thrust Modeling, A Simplified Thrust and Airflow Prediction Technique for Flight Test Performance Measurements," AIAA Paper 83-2751, Nov. 1983.